Journal of Mathematical Modeling and Fractional Calculus
https://acspublisher.com/journals/index.php/jmmfc
Received:20-11-2025, **Revised:** 14-12-2025,
Accepted: 10-03-2026, **Published:** 20-06-2026,
https://doi.org/10.48165/jmmfc.2026.3102,3(1),21-42

A CaputoŰFabrizio Fractional-Order TumorŰImmune Interaction Model with Treatment and Immunotherapy: Stability, Optimal Control, and Sensitivity Analysis

Ankita Dwivedi[a*], Santosh Verma[a*]

[a]Guru Ghasidas Vishwavidyalaya (A Central University)Bilaspur - 495009, India.
Corresponding author Email: ankitadwivedi910@gmail.com, santoshverma30@yahoo.co.in

Abstract:

We present a fractional-order immune tumor interaction model that captures both tumor progression and treatment effects under Caputo Fabrizio (CF) derivatives (a non-singular kernel fractional derivative). The model divides the system into five key compartments: naive immune cells, effector immune cells, viable tumor cells, treatment-affected tumor cells and dead tumor cells. It incorporates tumor logistic growth, immune activation, proliferation, immunotherapy infusion, drug-mediated cytotoxicity, relapse, and clearance processes. The fractional formulation reflects memory and hereditary properties inherent in biological interactions. Mathematical analysis establishes equilibrium points, derives the basic reproduction number and determines stability conditions for tumor-free and coexistence states. Numerical simulations support the theoretical results and reveal the influence of fractional order and therapeutic parameters on tumor suppression and long-term immune control. This framework bridges rigorous mathematical modeling with clinically relevant insights, offering guidance for optimizing immunotherapy and improving treatment strategies.

Keywords: Caputo Fabrizio operator; Tumor Model , Stability, Optimal Control, Sensitivity analysis

1. Introduction

Mathematical modeling has long served as a powerful framework for exploring complex biological processes, particularly in the context of tumor–immune interactions [5, 19]. Models provide essential tools to investigate mechanisms of cancer progression, immune surveillance and therapeutic interventions, enabling quantitative predictions and guiding treatment strategies. Traditional integer-order models have established important foundations, but they often fail to capture memory effects and hereditary dynamics inherent in biological systems[11, 29]. These limitations have motivated the adoption of fractional-order differential equations (FDEs), which inherently account for nonlocality and history dependence [25, 28]. Such features make FDEs especially well-suited to describing the long-term, cumulative effects of immune responses against tumors.

Recent research has highlighted the utility of fractional-order models in capturing the complex interplay between tumor cells and the immune system. In particular, fractional frameworks have been shown to enhance the realism of tumor growth dynamics, immune surveillance and therapy modeling [1, 3]. Building upon these advances, we formulate a novel fractional-order solid tumor–immune interaction model with treatment and immunotherapy. The model incorporates five interacting compartments: naive immune cells (S), effector immune cells (E), tumor cells (C), treated tumor cells (T) and dead cells (D) [16]. By integrating therapeutic interventions into the tumor–immune framework, our approach captures both natural immune processes and clinical strategies for cancer management.

The originality of this study lies in merging fractional-order dynamics with rigorous mathematical analysis. Specifically, our contributions can be summarized as follows:

1. We derive the basic reproduction number $\mathscr{R}_0$ and establish its significance as a threshold parameter distinguishing between tumor eradication and persistence [19, 22].
2. We conduct local and global stability analyses using Jacobian methods and Lyapunov functionals adapted to the fractional-order setting [23, 28].

3. We design optimal treatment and immunotherapy strategies by applying PontryaginŠs Maximum Principle, thereby balancing tumor reduction with treatment costs [4, 21, 31].
4. We perform sensitivity analysis of $\mathscr{R}_0$ and tumor progression dynamics to identify critical biological and therapeutic parameters that govern system behavior [8].

Taken together, these contributions establish a comprehensive modeling framework that bridges theory and practice. By incorporating fractional-order dynamics, stability theory, optimal control, and sensitivity analysis, our model not only deepens theoretical understanding of tumor–immune interactions but also provides actionable insights for optimizing cancer treatment [5, 10]. And we plot the graph with the use of python.

2. Preliminaries

Caputo–Fabrizio Fractional Derivative and Integral Formulation

The Caputo–Fabrizio (CF) fractional derivative of order $\eta \in (0,1)$ for a function $X_i(t)$ is defined as :

$$^{CF}D_t^{\eta} X_i(t) = \frac{M(\eta)}{1-\eta} \int_0^t X_i'(\tau) \exp\left(-\frac{\eta}{1-\eta}(t-\tau)\right) d\tau, \tag{1}$$

where $M(\eta)$ is a normalization function with $M(0) = M(1) = 1$, and the kernel is non-singular and exponential.

Equivalently, the CF derivative can be expressed in integral form as:

$$X_i(t) = X_i(0) + \frac{1-\eta}{M(\eta)} \int_0^t \Psi_i(\tau, X_i(\tau)) \exp\left(-\frac{\eta}{1-\eta}(t-\tau)\right) d\tau, \tag{2}$$

where $\Psi_i(t, X_i(t))$ is the right-hand side of the governing differential equation for the i^{th} state variable.

3. Model Formulation

As Behzad Ghanbari, Sunil Kumar and Ranbir Kumar [16] gave a mathematical model describing the interaction between immune cells $x(t)$ and tumor cells $y(t)$ is given by :

$$\frac{dx}{dt} = x(x) + x(x,y) - x(x,y) - x(x), \quad \frac{dy}{dt} = y\phi(y) - y(x,y), \quad t \geq 0. \tag{3}$$

and we consider a tumorŰimmune interaction model with five compartments: healthy cells (S), effector cells (E), tumor cells (C), treated tumor cells (T), and dead cells (D). The ordinary model is formulated using standard derivatives, while the memoryŰdependent extension is captured via the CaputoŰFabrizio (CF) fractional derivative with order $0 < \alpha \leq 1$.

Ordinary model (ODE form)..

$$\begin{aligned}
\frac{dS}{dt} &= \lambda - \frac{kC}{h+C} S - \delta_S S, \\
\frac{dE}{dt} &= \frac{kC}{h+C} S + \tau + \frac{\gamma_e E C}{\zeta + C} - \delta_E E - \delta_{EC} E C, \\
\frac{dC}{dt} &= r_c C(1-\theta C) - \kappa E C - uC - \delta_C C + rT, \\
\frac{dT}{dt} &= uC - \left(\omega + \delta_T + \kappa_T E + r\right) T, \\
\frac{dD}{dt} &= \kappa E C + \kappa_T E T + \omega T + \delta_C C + \delta_T T - \chi D.
\end{aligned} \tag{4}$$

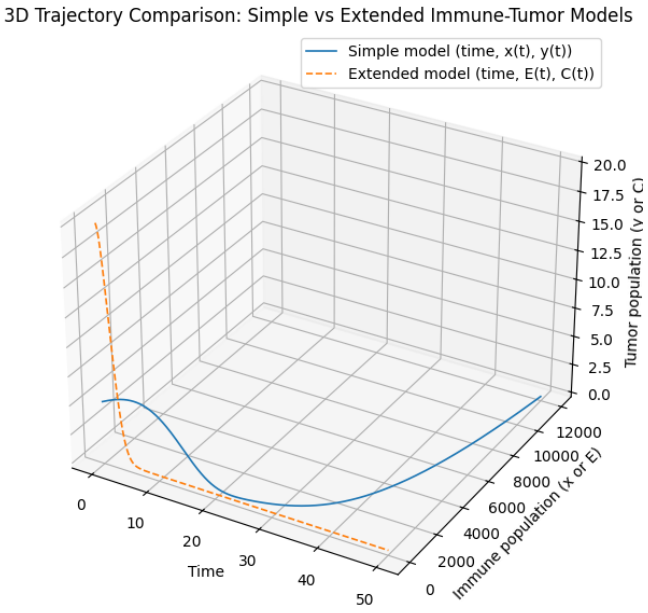

Figure 1: Comparison of 3^{rd} eq and 4^{th} eq.

In fig(1) shows that the simple model produces a long-term rise in the immune population while tumor declines to near zero (parameter-dependent).The extended model (approximated here as ODEs Ů the fractional derivative was approximated by standard time-stepping) shows more constrained tumor dynamics because of logistic growth, immuneŰtumor interactions, and treatment terms.

Fractional model (CF form).. Replacing the classical derivative with the CaputoŰFabrizio fractional operator gives:

$$\begin{aligned}
{}^{CF}S_t^{\alpha} &= \lambda - \frac{kC}{h+C}S - \delta_S S,\\
{}^{CF}E_t^{\alpha} &= \frac{kC}{h+C}S + \tau + \frac{\gamma_e E C}{\zeta + C} - \delta_E E - \delta_{EC} E C,\\
{}^{CF}C_t^{\alpha} &= r_c C(1-\theta C) - \kappa E C - uC - \delta_C C + rT,\\
{}^{CF}T_t^{\alpha} &= uC - \left(\omega + \delta_T + \kappa_T E + r\right) T,\\
{}^{CF}D_t^{\alpha} &= \kappa E C + \kappa_T E T + \omega T + \delta_C C + \delta_T T - \chi D.
\end{aligned} \tag{5}$$

Comparison.. Each compartment retains the same biological interactions under both formulations: - **1. Healthy cells** (S)**:** recruitment λ with loss due to tumor interaction and natural death. - **2. Effector cells** (E)**:** activated by tumor, supplied externally (τ), with natural death and tumor-induced apoptosis. - **3. cells** (C)**:** logistic growth with elimination via effector cells, treatment, and death. - **4. Treated tumor cells** (T)**:** arise from treatment of C, decay via immunity and natural loss. - **5. Dead cells** (D)**:** accumulate from tumor/treated tumor lysis and decay at rate χ.

The ODE system describes instantaneous dynamics, while the CFŰfractional system incorporates memory effects, making present states dependent on past interactions.

In fig.(2) line plots comparing each compartment under the ordinary model and the fractional CF model eq.(4,5).

4. Analysis of the Model

This section explores the well-posedness of the proposed model, focusing on the existence and uniqueness of solutions, as well as the preservation of positivity and boundedness of the system variables .

Existence and Uniqueness

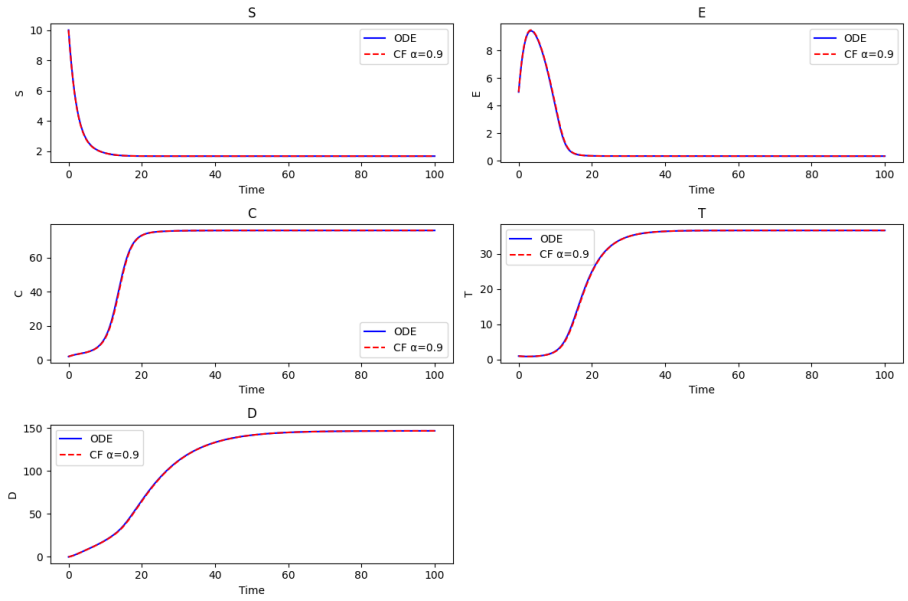

Figure 2: Compare of model the graph OD and CF with $\alpha = 0.9$.

Theorem 4.1. *There exists a unique solution of he proposed model eq.(5) for each non-negative condition.*

Proof. We are seeking for a sufficient condition for the presence and uniqueness of the proposed model solutions in the region $\Theta \times [0, \mathscr{T}]$, where $\Theta = (S,E,C,T,D) \in \mathbb{R}^5 \, from : \max ||S||, ||E||, ||C||, ||T||, ||D||$. The method employed is used consider a mapping
$\mathscr{G}(Y) = \mathscr{G}_1(Y), \mathscr{G}_2(Y), \mathscr{G}_3(Y), \mathscr{G}_4(Y), \mathscr{G}_5(Y)$. Where $Y = (S,E,C,T,D)$ and $\hat{Y} = (\hat{S},\hat{E},\hat{C},\hat{T},\hat{D})$

$$
\begin{aligned}
\mathscr{G}_1(Y) &= \lambda - \frac{kC}{h+C} S - \delta_S S, \\
\mathscr{G}_2(Y) &= \frac{kC}{h+C} S + \tau + \frac{\gamma_e E C}{\zeta + C} - \delta_E E - \delta_{EC} E C \\
\mathscr{G}_3(Y) &= r_c C (1 - \theta C) - \kappa E C - uC - \delta_C C + rT, \\
\mathscr{G}_4(Y) &= uC - \left(\omega + \delta_T + \kappa_T E + r\right) T, \\
\mathscr{G}_5(Y) &= \kappa E C + \kappa_T E T + \omega T + \delta_C C + \delta_T T - \chi D.
\end{aligned}
$$

$$
||\mathscr{G}(Y)-\mathscr{G}\hat{Y}|| = \begin{cases}
|\mathscr{G}_1(Y)-\mathscr{G}_1\hat{Y}|+|\mathscr{G}_2(Y)-\mathscr{G}_2\hat{Y}|+|\mathscr{G}_3(Y)-\mathscr{G}_3\hat{Y}|+|\mathscr{G}_4(Y)-\mathscr{G}_4\hat{Y}| \\
+|\mathscr{G}_5(Y)-\mathscr{G}_5\hat{Y}| \\
= |\lambda-\frac{kC}{h+C}S-\delta_S S-\lambda+\frac{k\hat{C}}{h+\hat{C}}\hat{S}+\delta_S\hat{S}| \\
|\frac{kC}{h+C}S+\tau+\frac{\gamma_e EC}{\zeta+C}-\delta_E E-\delta_{EC}EC-\frac{k\hat{C}}{h+\hat{C}}\hat{S}-\tau-\frac{\gamma_e\hat{E}\hat{C}}{\zeta+\hat{C}}+\delta_E\hat{E}+\delta_{EC}\hat{E}\hat{C}| \\
|r_c C(1-\theta C)-\kappa EC-uC-\delta_C C+rT-r_c\hat{C}(1-\theta\hat{C})+\kappa\hat{E}\hat{C}+u\hat{C} \\
+\delta_C\hat{C}-r\hat{T}|+|uC-\big(\omega+\delta_T+\kappa_T E+r\big)T-u\hat{C}+\big(\omega+\delta_T+\kappa_T\hat{E}+r\big)\hat{T}| \\
|\kappa EC+\kappa_T ET+\omega T+\delta_C C+\delta_T T-\chi D-\kappa\hat{E}\hat{C}-\kappa_T\hat{E}\hat{T}-\omega\hat{T}-\delta_C\hat{C} \\
-\delta_T\hat{T}+\chi\hat{D}|. \\
= |\frac{kC}{h+C}S-\frac{k\hat{C}}{h+\hat{C}}\hat{S}+\delta_S(S-\hat{S})|+|\frac{kC}{h+C}S-\frac{k\hat{C}}{h+\hat{C}}\hat{S}+\frac{\gamma_e EC}{\zeta+C}-\frac{\gamma_e\hat{E}\hat{C}}{\zeta+\hat{C}} \\
\delta_E(E-\hat{E})+\delta_{EC}(E-\hat{E})(C-\hat{C})|+|r_c C(1-\theta C)-r_c\hat{C}(1-\theta\hat{C}) \\
+K(E-\hat{E})(C-\hat{C})+u(C-\hat{C})+\delta_C(C-\hat{C})+r(T-\hat{T})| \\
|u(C-\hat{C})+\big(\omega+\delta_T+\kappa_T E+r\big)T-\big(\omega+\delta_T+\kappa_T\hat{E}+r\big)\hat{T}| \\
+|\kappa(E-\hat{E})(C-\hat{C})+\kappa_T(E-\hat{E})(T-\hat{T})+|\delta_C(C-\hat{C})+\delta_T(T-\hat{T}) \\
+\chi(D-\hat{D})| \\
= \underbrace{\frac{kM_C}{h+M_C}}_{\text{MM}\times S\text{ on }\Delta S}+\underbrace{\frac{kM_S}{h}}_{\text{MM}\times S\text{ on }\Delta C}+\underbrace{\delta_S}_{\Delta S} \\
+\underbrace{\gamma_e}_{\Delta E}+\underbrace{\frac{\gamma_e M_E}{4\zeta}}_{\Delta C}+\underbrace{\delta_E}_{\Delta E} \\
+\underbrace{\text{Lip}_C(\ell)}_{\text{logistic on }\Delta C}+\underbrace{K(M_E+M_C)}_{\Delta C,\ \Delta E}+\underbrace{u+\delta_C}_{\Delta C}+\underbrace{r}_{\Delta T} \\
+\underbrace{\big(\omega+\delta_T+r+\kappa_T M_E\big)}_{\Delta T}+\underbrace{\kappa_T M_T}_{\Delta E} \\
+\underbrace{\kappa(M_E+M_C)}_{\Delta C,\ \Delta E}+\underbrace{\delta_T}_{\Delta T}+\underbrace{\chi}_{\Delta D}.
\end{cases} \tag{6}
$$

$$
\big|\mathscr{G}(Y)-\mathscr{G}(\hat{Y})\big| \;\le\; L\|Y-\hat{Y}\|_1, \qquad \forall Y,\hat{Y}\in\Omega,
$$

where $\mathscr{G}(Y)$ is the collection of nonlinear and linear terms present in the system. This final expression provides a Lipschitz-type inequality. Such an inequality is instrumental in establishing uniqueness, stability, or convergence bounds for fractional-order systems. □

5. Positivity and Boundedness

With nonnegative initial data $(S,E,C,T,D)\big|_{t=0}\ge 0$, the vector field on each coordinate hyperplane points inward from eq.(5):

- If $S=0$: ${}^{CF}S=\lambda>0$.
- If $E=0$: ${}^{CF}E=\dfrac{kC}{h+C}S+\tau\ge 0$.
- If $C=0$: ${}^{CF}C=rT\ge 0$.
- If $T=0$: ${}^{CF}T=uC\ge 0$.
- If $D=0$: ${}^{CF}D=\kappa EC+\kappa_T ET+\omega T+\delta_C C+\delta_T T\ge 0$.

Hence the nonnegative orthant is positively invariant.

A simple linear functional is defined as

$$
W=S+E+C+T+D.
$$

Using the estimates

$$0 \le \frac{kC}{h+C} \le k, \qquad r_c C(1-\theta C) \le r_c C,$$

we obtain

$$^{CF}W \;\le\; \lambda + \tau + r_c C - \min\{\delta_S,\, \delta_E,\, \delta_C,\, \omega+\delta_T,\, \chi\}\,(S+E+C+T+D).$$

This inequality yields uniform boundedness of trajectories (by comparison with a scalar CF ODE). Thus, solutions exist globally, remain nonnegative and are bounded.

6. Stability Analysis

6.1. Local Stability Analysis

We consider the system eq.(5) and we use the Jacobian $J = \partial F/\partial(S,E,C,T,D)$ of system (5). Evaluate J at each equilibrium and apply the linearization theorem: an equilibrium is locally asymptotically stable [23, 27]iff every eigenvalue of the Jacobian has strictly negative real part.

Jacobian

$$J = \begin{pmatrix} -\frac{kC}{h+C} - \delta_S & 0 & -S\frac{kh}{(h+C)^2} & 0 & 0 \\ \frac{kC}{h+C} & \frac{\gamma_e C}{\zeta+C} - \delta_E - \delta_{EC}C & S\frac{kh}{(h+C)^2} + \gamma_e E\frac{\zeta}{(\zeta+C)^2} - \delta_{EC}E & 0 & 0 \\ 0 & -\kappa C & r_c(1-2\theta C) - \kappa E - u - \delta_C & r & 0 \\ 0 & -\kappa_T T & u & -(\omega+\delta_T+\kappa_T E+r) & 0 \\ 0 & \kappa C + \kappa_T T & \kappa E + \delta_C & \kappa_T E + \omega + \delta_T & -\chi \end{pmatrix}.$$

1. Equilibrium $E_0 = (0,0,0,0,0)$(null state).
Evaluate J at E_0 (put $S = E = C = T = D = 0$). The diagonal entries give the eigenvalues

$$\lambda_1 = -\delta_S, \qquad \lambda_2 = -\delta_E, \qquad \lambda_3 = r_c - u - \delta_C, \qquad \lambda_4 = -(\omega+\delta_T+r), \qquad \lambda_5 = -\chi.$$

Hence E_0 is locally asymptotically stable iff

$$\boxed{r_c - u - \delta_C < 0,}$$

(i.e. $r_c < u + \delta_C$), while the other diagonal terms are negative for positive parameters.

Biological meaning: The trivial state is stable only when intrinsic tumor growth r_c is overwhelmed by treatment engagement u and natural tumor loss δ_C.

2. Equilibrium $E_1 = (S_1,0,0,0,0)$ (healthy immune pool only) , $S_1 = \dfrac{\lambda}{\delta_S}$.
At E_1 the Jacobian is block lower-triangular: three obvious eigenvalues $\lambda = -\delta_S, -\delta_E, -\chi$ and a 2×2 (C,T) block

$$M_1 = \begin{pmatrix} a_1 & r \\ u & d_1 \end{pmatrix}, \qquad a_1 = r_c - u - \delta_C, \quad d_1 = -(\omega+\delta_T+r).$$

The two eigenvalues of M_1 lie in the left half-plane iff

$$\mathrm{tr}(M_1) = a_1 + d_1 < 0, \qquad \det(M_1) = a_1 d_1 - ru > 0.$$

Therefore E_1 is locally asymptotically stable iff

$$\boxed{r_c - u - \delta_C - (\omega+\delta_T+r) < 0 \quad \text{and} \quad (r_c - u - \delta_C)\cdot(-(\omega+\delta_T+r)) - ru > 0,}$$

plus $\delta_S, \delta_E, \chi > 0$.

Biological meaning: Treatment engagement u, treatment kill ω, natural deaths δ_C, δ_T and the coupling terms r must be such that net tumor growth and the relapse/feedback cannot overcome removal.

3. Equilibrium $E_2 = (S_2, E_2, 0, 0, 0)$ (immune-activated but no tumor), $S_2 = \dfrac{\lambda}{\delta_S}$, $E_2 = \dfrac{\tau}{\delta_E}$.
Same structure as E_1: eigenvalues $-\delta_S, -\delta_E, -\chi$ plus 2×2 block

$$M_2 = \begin{pmatrix} a_2 & r \\ u & d_2 \end{pmatrix}, \quad a_2 = r_c - u - \delta_C - \kappa\frac{\tau}{\delta_E}, \quad d_2 = -(\omega + \delta_T + r + \kappa_T\frac{\tau}{\delta_E}).$$

Stability conditions:

$$\boxed{\operatorname{tr}(M_2) = a_2 + d_2 < 0, \qquad \det(M_2) = a_2 d_2 - ru > 0.}$$

Biological meaning: Immune pressure (terms with κ, κ_T, τ) reduces effective tumor growth and assists stability.

4. Equilibrium E_3 / full endemic $E^* = (S^*, E^*, C^*, T^*, D^*)$.
If $D^* = 0$ the characteristic polynomial factorizes and $\lambda = -\chi$ is an eigenvalue. The remaining eigenvalues are roots of the quartic

$$p_4(\lambda) = \lambda^4 + b_1\lambda^3 + b_2\lambda^2 + b_3\lambda + b_4,$$

with

$$b_1 = -(a_{11} + a_{22} + a_{33} + a_{44}), \quad b_2, b_3, b_4 \text{ given by principal minors of } J_4.$$

Apply Routh–Hurwitz: all roots of p_4 have negative real parts iff

$$\boxed{b_1 > 0, \quad b_1 b_2 - b_3 > 0, \quad b_1 b_2 b_3 - b_1^2 b_4 - b_3^2 > 0, \quad b_4 > 0.}$$

For the full quintic characteristic polynomial of $J(E^*)$,

$$p(\lambda) = \lambda^5 + A_1\lambda^4 + A_2\lambda^3 + A_3\lambda^2 + A_4\lambda + A_5,$$

the equivalent Hurwitz conditions are

$$\boxed{\Delta_1 = A_1 > 0,\ \Delta_2 = A_1A_2 - A_3 > 0,\ \Delta_3 > 0,\ \Delta_4 > 0,\ A_5 > 0.}$$

Jacobian and eigenvalues at the tumor-free equilibrium

Theorem 6.1 (Linear stability principle)**.** *If all eigenvalues of J evaluated at an equilibrium E^* have strictly negative real parts, then E^* is locally asymptotically stable. If at least one eigenvalue has positive real part, E^* is unstable.*

Proof. **1. Tumor-free / null equilibrium $E_0 = (0,0,0,0,0)$**

Jacobian at E_0.. Substitute $S = E = C = T = D = 0$:

$$J(E_0) = \begin{pmatrix} -\delta_S & 0 & 0 & 0 & 0 \\ 0 & -\delta_E & 0 & 0 & 0 \\ 0 & 0 & r_c - u - \delta_C & r & 0 \\ 0 & 0 & u & -(\omega + \delta_T + r) & 0 \\ 0 & 0 & \delta_C & \omega + \delta_T & -\chi \end{pmatrix}.$$

Eigenvalues.. The matrix is block-triangular so eigenvalues are

$$\lambda_1 = -\delta_S, \quad \lambda_2 = -\delta_E, \quad \lambda_3, \lambda_4 \text{ (from the } 2\times 2 \text{ block on } C, T), \quad \lambda_5 = -\chi.$$

The 2×2 block for (C, T) is

$$M_0 = \begin{pmatrix} r_c - u - \delta_C & r \\ u & -(\omega + \delta_T + r) \end{pmatrix}.$$

Its eigenvalues satisfy $\lambda^2 - \operatorname{tr}(M_0)\lambda + \det(M_0) = 0$. □

Theorem 6.2. *E_0 is locally asymptotically stable iff*

$$\boxed{\delta_S > 0,\ \delta_E > 0,\ \chi > 0, \quad \textit{and} \quad \mathrm{tr}(M_0) < 0,\ \det(M_0) > 0}.$$

Equivalently, the necessary scalar conditions are

$$r_c < u + \delta_C \quad \textit{(to make the top-left of } M_0 \textit{ nonpositive in isolation)},$$

and the two Hurwitz inequalities for M_0.

Proof. The $\lambda_1, \lambda_2, \lambda_5$ are negative when $\delta_S, \delta_E, \chi > 0$. The remaining two eigenvalues are the roots of the characteristic polynomial of M_0. By the RouthŰHurwitz test for a quadratic, those two roots have negative real parts iff $\mathrm{tr}(M_0) < 0$ and $\det(M_0) > 0$. □

Biological remark: For the trivial tumour-free state to be stable the intrinsic tumor growth r_c must be sufficiently small relative to removal/engagement $u + \delta_C$ and the treatment/removal parameters (appear in $\mathrm{tr}(M_0), \det(M_0)$).

2. Semi-trivial equilibrium $E_1 = (S_1, 0, 0, 0, 0)$ with $S_1 = \dfrac{\lambda}{\delta_S}$

Jacobian at E_1.. Substitute $S = S_1,\ E = C = T = D = 0$. Nonzero entries:

$$J(E_1) = \begin{pmatrix} -\dfrac{k \cdot 0}{h+0} - \delta_S & 0 & -S_1 \dfrac{kh}{h^2} & 0 & 0 \\ 0 & -\delta_E & S_1 \dfrac{kh}{h^2} & 0 & 0 \\ 0 & 0 & r_c - u - \delta_C & r & 0 \\ 0 & 0 & u & -(\omega + \delta_T + r) & 0 \\ 0 & 0 & \delta_C & \omega + \delta_T & -\chi \end{pmatrix},$$

i.e. simplifying $h^2 = (h+0)^2$.

Eigenvalues and stability.. Again block triangular: eigenvalues

$$\lambda_1 = -\delta_S, \quad \lambda_2 = -\delta_E, \quad \lambda_5 = -\chi,$$

and the (C, T) block M_1 is identical in structure to M_0 (but coefficients unchanged). Thus E_1 is locally asymptotically stable iff $\delta_S, \delta_E, \chi > 0$ and the same two inequalities for M_1:

$$\mathrm{tr}(M_1) < 0, \qquad \det(M_1) > 0.$$

Interpretation: immune baseline S_1 does not affect the (C, T) linear block at $C = 0$ except via off-diagonal terms that vanish at $C = 0$, so stability reduces to the same tumor-treatment balance.

3. Immune-present tumor-free equilibrium $E_3 = (S_3, E_3, 0, 0, 0)$

We called this $E_3(S, E, 0, 0, 0)$. Here $S_3 = \dfrac{\lambda}{\delta_S}$, $E_3 = \dfrac{\tau}{\delta_E}$ (from the steady-state of S, E when $C = T = D = 0$).

Jacobian at E_3.. Substitute $S = S_3,\ E = E_3,\ C = T = D = 0$. Key nonzero entries:

$$J(E_3) = \begin{pmatrix} -\delta_S & 0 & -S_3 \dfrac{kh}{h^2} & 0 & 0 \\ 0 & -\delta_E & S_3 \dfrac{kh}{h^2} & 0 & 0 \\ 0 & 0 & r_c - u - \delta_C - \kappa E_3 & r & 0 \\ 0 & -\kappa_T \cdot 0 & u & -(\omega + \delta_T + r + \kappa_T E_3) & 0 \\ 0 & 0 & \delta_C & \omega + \delta_T & -\chi \end{pmatrix}.$$

Eigenvalues and stability conditions.. Eigenvalues: $-\delta_S, -\delta_E, -\chi$ plus the two eigenvalues of the shifted 2×2 block

$$M_3 = \begin{pmatrix} a_3 & r \\ u & d_3 \end{pmatrix}, \qquad a_3 = r_c - u - \delta_C - \kappa E_3, \quad d_3 = -\big(\omega + \delta_T + r + \kappa_T E_3\big).$$

Hence E_3 is locally asymptotically stable iff $\delta_S, \delta_E, \chi > 0$ and

$$\mathrm{tr}(M_3) = a_3 + d_3 < 0, \qquad \det(M_3) = a_3 d_3 - ru > 0.$$

Biological meaning: The presence of a nonzero effector pool E_3 improves stability by reducing effective tumor growth via κE_3 and making treated-cell removal larger via $\kappa_T E_3$.

4. Partially endemic candidate $E_4 = (S^*, E^*, C^*, 0, 0)$

This is the case $T^* = 0, D^* = 0$ with $C^* > 0$. Note: feasibility often fails unless $u = 0$ or other degenerate parameter combinations Ů check the equilibrium equations; but we treat stability formally.

Equilibrium feasibility.. From the T-equation at equilibrium:

$$0 = uC^* - (\omega + \delta_T + \kappa_T E^* + r)\cdot 0 \implies uC^* = 0.$$

Hence for $C^* > 0$ we need $u = 0$. If $u \neq 0$ a positive- C equilibrium with $T^* = 0$ cannot exist. If $u = 0$ proceed with the following.

Jacobian at E_4.. Evaluate J at $(S^*, E^*, C^*, 0, 0)$. The structure is

$$J(E_4) = \begin{pmatrix} a_{11} & 0 & a_{13} & 0 & 0 \\ a_{21} & a_{22} & a_{23} & 0 & 0 \\ 0 & a_{32} & a_{33} & r & 0 \\ 0 & 0 & u & a_{44} & 0 \\ 0 & a_{52} & a_{53} & a_{54} & -\chi \end{pmatrix},$$

with entries as in the general Jacobian evaluated at the equilibrium.

Eigenvalues and reduced test.. Because the last column is zero except $-\chi$ at $(5,5)$, $-\chi$ is an eigenvalue. The remaining eigenvalues are roots of the quartic $\det(\lambda I_4 - J_4)$ with J_4 the top-left 4×4 block. Use the quartic RouthŰHurwitz conditions: let

$$p_4(\lambda) = \lambda^4 + b_1\lambda^3 + b_2\lambda^2 + b_3\lambda + b_4,$$

then the necessary and sufficient conditions for all roots to have negative real parts are

$$b_1 > 0, \quad b_1 b_2 - b_3 > 0, \quad b_1 b_2 b_3 - b_1^2 b_4 - b_3^2 > 0, \quad b_4 > 0.$$

Compute the b_i from principal minors of J_4 (substitute numerical parameter values to check).

Note on feasibility: In most biologically realistic parameter sets where $u > 0$, E_4 does not exist. If it exists (e.g. $u = 0$), apply the quartic test.

5. Endemic with treated tumor but no dead cells $E_5 = (S^*, E^*, C^*, T^*, 0)$

We consider the equilibrium point of the form

$$E_5 = (S^*, E^*, C^*, T^*, 0),$$

where the right-hand sides of the system are set equal to zero.

1. Susceptible cells (S):.

$$0 = \lambda - \frac{kC}{h+C} S - \delta_S S,$$

which gives

$$S^*(C) = \frac{\lambda}{\delta_S + \dfrac{kC}{h+C}} = \frac{\lambda(h+C)}{\delta_S(h+C)+kC}.$$

2. Effector cells (E):.

$$0 = \frac{kC}{h+C} S + \tau + \frac{\gamma_e E C}{\zeta + C} - \delta_E E - \delta_{EC} E C,$$

hence

$$E^*(C) = \frac{\dfrac{kC}{h+C} S^*(C) + \tau}{\delta_E + \delta_{EC} C - \dfrac{\gamma_e C}{\zeta + C}}.$$

3. Treated tumor cells (T):.

$$0 = uC - \left(\omega + \delta_T + \kappa_T E + r\right) T,$$

so that

$$T^*(C) = \frac{uC}{\omega + \delta_T + \kappa_T E^*(C) + r}.$$

4. Tumor cells (C):.

$$0 = r_c C(1 - \theta C) - \kappa E C - uC - \delta_C C + rT.$$

For $C > 0$, this reduces to the scalar equation

$$F(C) \equiv r_c(1 - \theta C) - \kappa E^*(C) - u - \delta_C + \frac{ru}{\omega + \delta_T + \kappa_T E^*(C) + r} = 0.$$

5. Dead cells (D):. Since we require $D^* = 0$, this component vanishes in E_5.

Therefore, the endemic equilibrium E_5 is given by:

$$E_5 = \left(\frac{\lambda(h+C^*)}{\delta_S(h+C^*)+kC^*}, \frac{\dfrac{kC^*}{h+C^*} S^* + \tau}{\delta_E + \delta_{EC} C^* - \dfrac{\gamma_e C^*}{\zeta + C^*}}, C^*, \frac{uC^*}{\omega + \delta_T + \kappa_T E^* + r}, 0 \right),$$

where $C^* > 0$ is any positive solution of $F(C) = 0$.

Feasibility conditions:.

- $C^* > 0$ solves $F(C) = 0$.
- $\delta_S(h+C^*) + kC^* > 0$,
- $\delta_E + \delta_{EC} C^* - \dfrac{\gamma_e C^*}{\zeta + C^*} > 0$,
- $\omega + \delta_T + \kappa_T E^* + r > 0$.

Under these conditions, $S^*, E^*, T^* > 0$ and $D^* = 0$.

6. Full endemic equilibrium $E_6 = (S^*, E^*, C^*, T^*, D^*)$

$$
\begin{aligned}
S^* &= \frac{\lambda(h+C^*)}{\delta_S(h+C^*)+kC^*},\\
E^* &= \frac{\dfrac{kC^*}{h+C^*}S^*(C^*)+\tau}{\delta_E+\delta_{EC}C^*-\dfrac{\gamma_e C^*}{\zeta+C^*}},\\
T^* &= \frac{uC^*}{\omega+\delta_T+\kappa_T E^*(C^*)+r},\\
D^* &= \frac{\kappa E^*(C^*)C^*+\kappa_T E^*(C^*)T^*(C^*)+\omega T^*(C^*)+\delta_C C^*+\delta_T T^*(C^*)}{\chi},\\
&C^* \text{ is any positive root of } F(C)=0.
\end{aligned}
$$

Feasibility (positivity) conditions. To ensure $S^*, E^*, C^*, T^*, D^* > 0$ require:

- $C^* > 0$ solves $F(C) = 0$,
- $\delta_S(h+C^*)+kC^* > 0$ (so $S^* > 0$),
- $\delta_E+\delta_{EC}C^*-\dfrac{\gamma_e C^*}{\zeta+C^*} > 0$ (so denominator in E^* is positive),
- $\omega+\delta_T+\kappa_T E^*(C^*)+r > 0$ (so $T^* > 0$),
- numerators of E^* and D^* positive (this typically holds if $\tau \geq 0$ and parameters are positive). We explained in fig.(4) [1, 2, 3].

6.2. Global Stability of the Tumor-Free Equilibrium E_0

Because the compartment D does not feed back into (S,E,C,T) and only decays when its sources vanish, it suffices to stabilize the subsystem (C,T) and then show convergence of $(S,E) \to (S^*,E^*)$which explained in fig(5) [14].

Step 1. Lyapunov functional for the tumor block.. Consider the linear Lyapunov functional

$$V(C,T) = C+\xi T, \qquad \xi > 0 \ \text{(to be chosen)}.$$

From the model eq.(2),

$$
\begin{aligned}
{}^{CF}V &= \Big[r_c C(1-\theta C)-\kappa EC-uC-\delta_C C+rT\Big]+\xi\Big[uC-(\omega+\delta_T+\kappa_T E+r)T\Big]\\
&\leq \underbrace{(r_c-u-\delta_C+\xi u)}_{=A}C+\underbrace{(r-\xi(\omega+\delta_T+r))}_{=B}T,
\end{aligned}
$$

where the inequality follows by dropping the nonpositive terms $-r_c\theta C^2$, $-\kappa EC$, and $-\xi\kappa_T ET$ (this makes the argument global, independent of E).

Step 2. Choice of parameter ξ.. When we select

$$\xi = \frac{r}{\omega+\delta_T+r} \quad \Longrightarrow \quad B = 0.$$

Then

$${}^{CF}V \leq (r_c-\delta_C-u+\xi u)C.$$

Step 3. Effective net tumor growth.. Define the *effective net tumor growth rate at the boundary* $E = 0$ by

$$\Gamma = r_c - \delta_C - u\,\frac{\omega + \delta_T}{\omega + \delta_T + r}.$$

Indeed, with the chosen ξ,

$$r_c - u - \delta_C + \xi u = r_c - \delta_C - u\Big(1 - \tfrac{r}{\omega+\delta_T+r}\Big) = r_c - \delta_C - u\,\frac{\omega + \delta_T}{\omega + \delta_T + r} = \Gamma.$$

Hence

$$^{CF}V \le \Gamma C \le \Gamma V, \qquad \text{since } 0 \le C \le V.$$

Step 4. Global condition.. If

$$\Gamma < 0 \iff r_c < \delta_C + u\,\frac{\omega + \delta_T}{\omega + \delta_T + r},$$

then $^{CF}V \le \Gamma V$ with $\Gamma < 0$. Thus $V(t)$ is strictly decreasing unless $C = 0$. By the CF version of LaSalleŠs invariance principle (for nonsingular exponential kernels), the largest invariant set in $\{^{CF}V = 0\}$ is

$$\{(C,T) : C = 0, T = 0\}.$$

Therefore

$$(C(t),T(t)) \to (0,0) \qquad \text{globally as } t \to \infty.$$

Step 5. Convergence of (S,E,D)*..* With $(C(t),T(t)) \to (0,0)$, the dynamics for (S,E) asymptotically reduce to linear CF equations:

$$^{CF}S = \lambda - \delta_S S + o(1), \qquad ^{CF}E = \tau - \delta_E E + o(1).$$

Solutions of equations of the form $^{CF}x = a - bx$ converge exponentially to $x^* = a/b$ for $b > 0$. Hence

$$S(t) \to S^* = \frac{\lambda}{\delta_S}, \qquad E(t) \to E^* = \frac{\tau}{\delta_E}.$$

Finally, since $C, T \to 0$,

$$^{CF}D = -\chi D + \kappa EC + \kappa_T ET + \omega T + \delta_C C + \delta_T T \;\longrightarrow\; -\chi D,$$

so that $D(t) \to 0$.

Theorem 6.3 (Global Tumor-Free Stability)**.** *For the CF system, suppose*

$$r_c < \delta_C + u\,\frac{\omega + \delta_T}{\omega + \delta_T + r}.$$

Then the tumor-free equilibrium [21]

$$E_0 = \left(\frac{\lambda}{\delta_S},\, \frac{\tau}{\delta_E},\, 0,\, 0,\, 0\right)$$

is globally asymptotically stable in the nonnegative orthant: every nonnegative, bounded solution satisfies

$$(S(t),E(t),C(t),T(t),D(t)) \;\longrightarrow\; \left(\frac{\lambda}{\delta_S},\, \frac{\tau}{\delta_E},\, 0,\, 0,\, 0\right) \quad \text{as } t \to \infty.$$

Theorem 6.4 (Global stability of the disease–free equilibrium)**.** *Let* $E_0 = (S_0,0,0,0,0)$ *denote the disease–free equilibrium with* $S_0 = \dfrac{\lambda}{\delta_S}$*. Construct the usual next–generation matrices* F *and* V *for the infected subsystem (we choose infected variables* $y = (E,C,T,D)$*), evaluated at the DFE (so* $S = S_0$*,* $E = C = T = D = 0$*) and let*

$$\mathscr{R}_0 = \rho(FV^{-1})$$

be the basic reproduction number (spectral radius of FV^{-1}*). If*

$$\mathscr{R}_0 < 1,$$

then the DFE E_0 *is globally asymptotically stable in the nonnegative invariant set [23].*

Proof. The proof proceeds in three steps: Linearization/next–generation, construction of a Lyapunov-type estimate for the infected subsystem, and a comparison/monotonically argument adapted to the Caputo–Fabrizio derivative.

Step 1. linear infected subsystem at the DFE. Write the infected subsystem in the form

$$^{CF}y = \mathscr{F}(x) - \mathscr{V}(x),$$

where $\mathscr{F}$ collects *new infection* terms and $\mathscr{V}$ collects transfer/removal terms. Evaluate the linearization at the DFE to obtain

$$^{CF}y \;=\; (F-V)y + G(y,S),$$

where F,V are nonnegative matrices (with V an M-matrix) and $G(y,S)$ contains higher-order (at least quadratic) terms in y and terms proportional to $(S-S_0)y$. By construction FV^{-1} is nonnegative and $\mathscr{R}_0 = \rho(FV^{-1})$.

Step 2. linear comparison and exponential-type decay under $\mathscr{R}_0 < 1$. Since V is an M-matrix, $-V$ is a Metzler matrix with negative diagonal entries. The matrix $M = V - F$ is a Metzler matrix whose spectral bound satisfies

$$s(M) < 0 \quad \Longleftrightarrow \quad \rho(FV^{-1}) < 1.$$

When $\mathscr{R}_0 < 1$ we thus have $s(M) < 0$ i.e. the linear ODE system

$$^{CF}z = Mz$$

is exponentially (in the classical sense) stable. For the Caputo–Fabrizio derivative the linear scalar comparison principle and the linearity of the CF operator imply that solutions of the linear system satisfy an exponential-type decay bound (then we see standard CF linear stability results): there exist constants $K, \mu > 0$ such that

$$\|z(t)\| \le Ke^{-\mu t}\|z(0)\|, \qquad t \ge 0.$$

Step 3. nonlinearity control and global attractivity. Return to the full infected equation

$$^{CF}y = My + G(y,S).$$

Because $G(y,S) = o(\|y\|)$ as $\|y\| \to 0$ and G is nonnegative-order higher (it contains only quadratic and mixed terms), there exists a neighborhood U of the origin in which G is dominated by $\varepsilon\|y\|$ with $\varepsilon > 0$ arbitrarily small. Choose ε such that $s(M) + \varepsilon < 0$. Then within U the linear dissipativity dominates the nonlinear terms, and solutions enter and remain in U and decay to 0.

To extend from local to global attractivity, use the fact that the full system is cooperative (the infected subsystem has nonnegative off-diagonal partial derivatives when $S \ge 0$) and that solutions are bounded. For cooperative bounded systems one may apply the *comparison principle*: for any initial data $y(0) \ge 0$ there exists a comparison solution $\bar{y}(t)$ solving the linear system

$$^{CF}\bar{y} = (M + \varepsilon I)\bar{y}, \qquad \bar{y}(0) = y(0),$$

with $(M+\varepsilon I)$ still Hurwitz for suitably small $\varepsilon > 0$. The comparison principle yields $0 \le y(t) \le \bar{y}(t)$ componentwise for all $t \ge 0$, and hence $y(t) \to 0$ as $t \to \infty$. Because $S(t)$ obeys a decoupled scalar equation with globally attracting equilibrium S_0 when $y(t) \to 0$, we get $S(t) \to S_0$. Therefore the whole state $x(t) \to E_0$ as $t \to \infty$ for any nonnegative initial data.Hence E_0 is globally asymptotically stable whenever $\mathscr{R}_0 < 1$. □

7. Basic reproduction number $\mathscr{R}_0$

We take the tumor [24, 31, 32, 33] related infected block as $x = (C,T)^\top$. The tumor-free equilibrium (TFE) is

$$E_0 = \Big(S^*, E^*, 0, 0, 0\Big), \qquad S^* = \frac{\lambda}{\delta_S}, \quad E^* = \frac{\tau}{\delta_E}.$$

Linearizing the (C,T)-subsystem about E_0 gives

$$^{CF}C = r_c C - (\kappa E^* + u + \delta_C)C + rT + (\text{higher order terms}),$$

$$^{CF}T = uC - (\omega + \delta_T + \kappa_T E^* + r)T + (\text{higher order terms}).$$

Following the nextŰgeneration matrix [9, 10, 11] approach we split the linearized right-hand side as

$$^{CF}x = F(x) - V(x), \qquad x = (C,T)^\top,$$

where $F_i(x)$ are rates of appearance of *new* tumor cells in compartment i produced by infected compartments and $V(x)$ collects all other transfers, removals and transfers between infected compartments.

A natural and standard choice is

$$F(x) \;=\; \begin{pmatrix} r_c C \\ 0 \end{pmatrix}, \qquad V(x) \;=\; \begin{pmatrix} (\kappa E^* + u + \delta_C)\,C - r\,T \\ (\omega + \delta_T + \kappa_T E^* + r)\,T - u\,C \end{pmatrix}.$$

The Jacobians of F and V at E_0 (w.r.t. $x = (C,T)$) are

$$F \;=\; \begin{pmatrix} r_c & 0 \\ 0 & 0 \end{pmatrix}, \qquad V \;=\; \begin{pmatrix} u + \delta_C + \kappa E^* & -r \\ -u & \omega + \delta_T + \kappa_T E^* + r \end{pmatrix}.$$

The next-generation matrix is

$$\mathscr{K} \;=\; F\,V^{-1}.$$

A direct computation (using the formula for the inverse of a 2×2 matrix) yields the single nonzero eigenvalue of $\mathscr{K}$:

$$\mathscr{K} = \begin{pmatrix} \dfrac{r_c\big(\omega + \delta_T + \kappa_T E^* + r\big)}{\big(u + \delta_C + \kappa E^*\big)\big(\omega + \delta_T + \kappa_T E^* + r\big) - r\,u} & 0 \\ 0 & 0 \end{pmatrix}.$$

Hence the basic reproduction number [18, 32] (spectral radius of $\mathscr{K}$) is which explained fig(6)

$$\boxed{\mathscr{R}_0 \;=\; \frac{r_c\big(\omega + \delta_T + \kappa_T E^* + r\big)}{\big(u + \delta_C + \kappa E^*\big)\big(\omega + \delta_T + \kappa_T E^* + r\big) - r\,u}}.$$

8. Optimal control problem

We consider the controlled (classical, integer-order) version of the model of eq.(2) on $t \in [0,t_f]$ with given nonnegative initial data $(S(0),E(0),C(0),T(0),D(0))$. The controls satisfy measurable bounds

$$0 \le u(t) \le u_{\max}, \qquad 0 \le \tau(t) \le \tau_{\max}.$$

Choose the following objective functional (typical quadratic-cost formulation):

$$J(u,\tau) = \int_0^{t_f} \Big(w_1 C(t) + w_2 T(t) + \tfrac{1}{2} v_1 u(t)^2 + \tfrac{1}{2} v_2 \tau(t)^2 \Big)\, dt + \Phi\big(S(t_f),E(t_f),C(t_f),T(t_f),D(t_f)\big), \qquad (7)$$

where $w_i, v_j > 0$ are weighting parameters and Φ is a smooth terminal cost (we will often take $\Phi \equiv 0$, but include it for generality). The aim is

$$\min_{(u,\tau)\in\mathscr{U}} J(u,\tau)$$

where $\mathscr{U}$ is the set of measurable.

Hamiltonian and adjoint equations (Pontryagin).. Define the Hamiltonian

$$\begin{aligned} H = {} & w_1 C + w_2 T + \tfrac{1}{2} v_1 u^2 + \tfrac{1}{2} v_2 \tau^2 + \lambda_S \Big(\lambda - \frac{kC}{h+C} S - \delta_S S \Big) \\ & + \lambda_E \Big(\frac{kC}{h+C} S + \tau + \frac{\gamma_e E C}{\zeta + C} - \delta_E E - \delta_{EC} E C \Big) \\ & + \lambda_C \Big(r_c C(1-\theta C) - \kappa E C - u C - \delta_C C + r T \Big) \\ & + \lambda_T \Big(u C - (\omega + \delta_T + \kappa_T E + r) T \Big) \\ & + \lambda_D \Big(\kappa E C + \kappa_T E T + \omega T + \delta_C C + \delta_T T - \chi D \Big), \end{aligned}$$

where $\lambda_S, \lambda_E, \lambda_C, \lambda_T, \lambda_D$ are the costate (adjoint) variables.

Pontryagin's necessary conditions give the adjoint (costate) system (backward in time)

$$\dot{\lambda}_i(t) = -\frac{\partial H}{\partial x_i}, \qquad \lambda_i(t_f) = \frac{\partial \Phi}{\partial x_i}\Big|_{t_f},$$

for $x = (S, E, C, T, D)$. Computing the partial derivatives yields (all functions evaluated at the current state; primes denote derivatives w.r.t. the indicated variable):

$$\begin{aligned}
\dot{\lambda}_S &= -\frac{\partial H}{\partial S} = -\lambda_S\Big(-\frac{kC}{h+C} - \delta_S\Big) - \lambda_E\Big(\frac{kC}{h+C}\Big),\\
\dot{\lambda}_E &= -\frac{\partial H}{\partial E} = -\lambda_E\Big(\frac{\gamma_e C}{\zeta + C} - \delta_E - \delta_{EC}C\Big) - \lambda_C\big(-\kappa C\big) - \lambda_T\big(-\kappa_T T\big) - \lambda_D\big(\kappa C + \kappa_T T\big),\\
\dot{\lambda}_C &= -\frac{\partial H}{\partial C} = -w_1 - \lambda_S\Big(-S\phi'(C)\Big) - \lambda_E\Big(S\phi'(C) + \gamma_e E\frac{\zeta}{(\zeta+C)^2} - \delta_{EC}E\Big)\\
&\quad - \lambda_C\big(r_c(1-2\theta C) - \kappa E - u - \delta_C\big) - \lambda_T\big(u\big) - \lambda_D\big(\kappa E + \delta_C\big),\\
\dot{\lambda}_T &= -\frac{\partial H}{\partial T} = -w_2 - \lambda_C r - \lambda_T\big(-(\omega + \delta_T + \kappa_T E + r)\big) - \lambda_D(\kappa_T E + \omega + \delta_T),\\
\dot{\lambda}_D &= -\frac{\partial H}{\partial D} = -\lambda_D(-\chi) = \chi\,\lambda_D,
\end{aligned}$$

where $\phi(C) = \dfrac{kC}{h+C}$ and $\phi'(C) = \dfrac{kh}{(h+C)^2}$. The terminal conditions are $\lambda_i(t_f) = \partial\Phi/\partial x_i\big|_{t_f}$; for free end-state with $\Phi \equiv 0$ we take $\lambda_i(t_f) = 0$.

Characterisation of the optimal controls.. The optimal controls [7, 20] $u^*(t), \tau^*(t)$ minimize the Hamiltonian a.e.; since the Hamiltonian [11, 15]is convex in the controls (quadratic terms) the necessary condition is $\partial H/\partial u = 0,\ \partial H/\partial \tau = 0$ together with projection onto the admissible set explained in fig(7) .

Compute

$$\frac{\partial H}{\partial u} = v_1 u - \lambda_C C + \lambda_T C, \qquad \frac{\partial H}{\partial \tau} = v_2\tau + \lambda_E.$$

Thus the unconstrained minimisers are

$$u^{\text{un}}(t) = \frac{(\lambda_C(t) - \lambda_T(t))\,C(t)}{v_1}, \qquad \tau^{\text{un}}(t) = -\frac{\lambda_E(t)}{v_2}.$$

Projecting onto the control bounds $[0, u_{\max}]$ and $[0, \tau_{\max}]$ gives the optimal feedback laws

$$\boxed{u^*(t) \;=\; \min\Big\{u_{\max},\, \max\Big\{0,\, \frac{(\lambda_C - \lambda_T)C}{v_1}\Big\}\Big\}, \qquad \tau^*(t) \;=\; \min\Big\{\tau_{\max},\, \max\Big\{0,\, -\frac{\lambda_E}{v_2}\Big\}\Big\}.}$$

9. Stability and Sensitivity Analysis

1. Tumor-free equilibrium (DFE). Setting $C = 0$, the steady state is

$$S_0 = \tfrac{\lambda}{\delta_S}, \quad E_0 = \tfrac{\tau}{\delta_E}, \quad C_0 = T_0 = D_0 = 0,$$

i.e.,

$$E_0 = \Big(\tfrac{\lambda}{\delta_S},\ \tfrac{\tau}{\delta_E},\ 0, 0, 0\Big).$$

2. Linearized tumor growth. For small C:

$$\dot{C} \approx (r_c - \kappa E_0 - u - \delta_C)C + rT, \qquad \dot{T} \approx uC - \alpha T,$$

with

$$\alpha = \omega + \delta_T + r + \kappa_T E_0, \quad E_0 = \tfrac{\tau}{\delta_E}.$$

At quasiŰsteady state $T \approx \frac{u}{\alpha} C$, giving

$$\dot{C} \approx \Lambda_C C, \quad \Lambda_C = r_c - \kappa E_0 - u - \delta_C + \frac{ru}{\alpha}.$$

If $\Lambda_C > 0$, tumors grow; if $\Lambda_C < 0$, they decay.

3. Sensitivity index. For $F(p)$, we explained in fig(8) [8, 17, 26]

$$\varphi_p(F) = \frac{p}{F} \frac{\partial F}{\partial p}.$$

4. Sensitivity of Λ_C.

$$\Lambda_C = r_c - \kappa \frac{\tau}{\delta_E} - u - \delta_C + \frac{ru}{\alpha}, \quad \alpha = \omega + \delta_T + r + \kappa_T \frac{\tau}{\delta_E}.$$

Partial derivatives:

$$\begin{aligned}
&\frac{\partial \Lambda_C}{\partial r_c} = 1, \quad \frac{\partial \Lambda_C}{\partial \kappa} = -E_0, \quad \frac{\partial \Lambda_C}{\partial \tau} = -\frac{\kappa}{\delta_E} - \frac{\kappa_T r u}{\delta_E \alpha^2}, \\
&\frac{\partial \Lambda_C}{\partial \delta_E} = \frac{\kappa \tau}{\delta_E^2} + \frac{\kappa_T r \tau u}{\delta_E^2 \alpha^2}, \quad \frac{\partial \Lambda_C}{\partial u} = \frac{r}{\alpha} - 1, \quad \frac{\partial \Lambda_C}{\partial \delta_C} = -1, \\
&\frac{\partial \Lambda_C}{\partial r} = \frac{u}{\alpha} - \frac{ru}{\alpha^2}, \quad \frac{\partial \Lambda_C}{\partial \omega} = -\frac{ru}{\alpha^2}, \quad \frac{\partial \Lambda_C}{\partial \delta_T} = -\frac{ru}{\alpha^2}, \quad \frac{\partial \Lambda_C}{\partial \kappa_T} = -\frac{r \tau u}{\delta_E \alpha^2}.
\end{aligned}$$

Normalized indices:

Table 1: Normalized sensitivity indices of Λ_C

Parameter	Sensitivity Index $\varphi_p(\Lambda_C)$
r_c	$\frac{r_c}{\Lambda_C}$
κ	$-\frac{\kappa E_0}{\Lambda_C}$
τ	$\frac{\tau}{\Lambda_C}\left(-\frac{\kappa}{\delta_E} - \frac{\kappa_T r u}{\delta_E \alpha^2}\right)$
δ_E	$\frac{1}{\Lambda_C}\left(\frac{\kappa \tau}{\delta_E} + \frac{\kappa_T r \tau u}{\delta_E \alpha^2}\right)$
u	$\frac{u}{\Lambda_C}\left(\frac{r}{\alpha} - 1\right)$
δ_C	$-\frac{\delta_C}{\Lambda_C}$
r	$\frac{ru}{\Lambda_C}\left(\frac{1}{\alpha} - \frac{r}{\alpha^2}\right)$
ω	$-\frac{\omega}{\Lambda_C}\frac{ru}{\alpha^2}$
δ_T	$-\frac{\delta_T}{\Lambda_C}\frac{ru}{\alpha^2}$
κ_T	$-\frac{\kappa_T}{\Lambda_C}\frac{r \tau u}{\delta_E \alpha^2}$

10. Numerical Analysis

To complement the theoretical results, we perform numerical simulations of the proposed fractional-order tumorŰimmune interaction model. The system of Caputo fractional-order differential equations is solved using the PredictorŰCorrector AdamsŰBashforthŰMoulton (ABM) scheme which is well-suited for capturing memory-dependent dynamics. Parameters are chosen from established tumorŰimmune interaction studies, ensuring biological plausibility, with initial conditions representing small tumor populations under therapeutic intervention. Unless otherwise specified, the fractional order is set to $\alpha = 0.95$, reflecting memory effects while remaining close to the classical case. Simulations without treatment confirm the threshold property of the basic reproduction number $\mathscr{R}_0$, where tumor cells persist or vanish depending on whether $\mathscr{R}_0$ is above or below unity. Introducing optimal treatment and immunotherapy, derived from PontryaginŠs Maximum Principle, demonstrates that combined therapies outperform single interventions, with fractional-order memory effects prolonging immune responses and enhancing tumor clearance. Sensitivity simulations further highlight tumor growth rate and treatment efficacy as the most influential parameters, in agreement with analytical sensitivity indices. Overall, the numerical results validate the theoretical framework, emphasizing that fractional-order dynamics significantly affect tumor progression, therapeutic efficiency, and long-term immune response.And all figure plot with the use of Tables(2, 3, 4)

Table 2: Model parameters: description and plausible values for a solid tumor immune response model

Parameter	Description	Typical value (human/day)
λ	Baseline influx of naive immune cells S	1×10^3 cells/day (influx)
k	Activation rate of S by tumor antigen	0.01–0.1 per tumor cell per day
h	Half-saturation constant for activation	10^6 tumor cells
δ_S	Natural death rate of S	0.05–0.1 day^{-1}
τ	Constant immunotherapy infusion into E	100 cells/day (e.g. dosing rate)
γ_e	Max tumor-stimulated proliferation rate of E	0.1–0.5 day^{-1}
ζ	Half-saturation constant for E expansion	10^6 tumor cells
δ_E	Natural death rate of effector immune cells E	0.1–0.2 day^{-1}
δ_{EC}	Tumor-induced death rate coefficient of E	1×10^{-6} per tumor cell per day
r_c	Intrinsic tumor growth rate of C	0.2–1.0 day^{-1}
θ	Inverse carrying-capacity parameter of C	1×10^{-9} per cell
κ	Immune killing efficacy on tumor cells C	1×10^{-7} per immune cell per day
u	Treatment engagement rate of C into T	0.05–0.2 day^{-1}
δ_C	Natural death rate of tumor cells	0.01–0.05 day^{-1}
r	Relapse/reversion rate from T back to C	0.01–0.05 day^{-1}
ω	Drug-mediated killing rate of T	0.5–1.0 day^{-1}
δ_T	Natural death rate of T	0.02–0.1 day^{-1}
κ_T	Immune killing efficacy on treated cells T	5×10^{-8} per immune cell per day
χ	Clearance rate of dead cells D	0.2–0.5 day^{-1}

Table 3: Description of state variables and their values

Variable	Description	Value
$S(t)$	Density of susceptible (naive) immune cells at time t	7,696.2643
$E(t)$	Density of activated/effector immune cells at time t	0.64833107
$C(t)$	Density of viable tumor cells at time t	7.471427272×10^8
$T(t)$	Density of treatment-affected tumor cells at time t	8.89455593×10^7
$D(t)$	Density of dead/cleared tumor cells at time t	2.698863891×10^8

Table 4: Normalized sensitivity indices of Λ_C with respect to key parameters

Parameter	Description	Value (day^{-1} or cells/day)	Sensitivity Index $\varphi_p(\Lambda_C)$
r_c	Tumor growth rate	0.6	φ_{r_c}
κ	Immune killing rate on C	1×10^{-7}	φ_κ
τ	Immunotherapy infusion rate	100	φ_τ
δ_E	Natural death rate of E	0.15	φ_{δ_E}
u	Treatment engagement rate	0.125	φ_u
δ_C	Tumor natural death rate	0.03	φ_{δ_C}
r	Relapse/reversion rate	0.03	φ_r
ω	Drug-mediated killing rate	0.75	φ_ω
δ_T	Natural death rate of T	0.06	φ_{δ_T}
κ_T	Immune killing on T	5×10^{-8}	φ_{κ_T}

Fig(3)
Comparison of model.

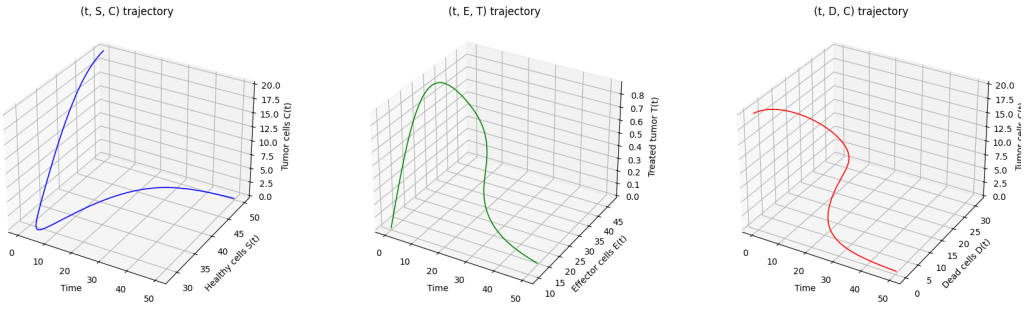

Figure 3: Compare of model between the t with S, E, C, T, D.

In fig(3) shows the left side (t,S,C): How healthy cells $S(t)$ interact with tumor cells $C(t)$ over time. In middle side (t,E,T): How effector cells $E(t)$ respond against treated tumor cells $T(t)$. In right side (t,D,C): The relationship between dead cells $D(t)$ and tumor cells $C(t)$.

Fig(4) Local Stability

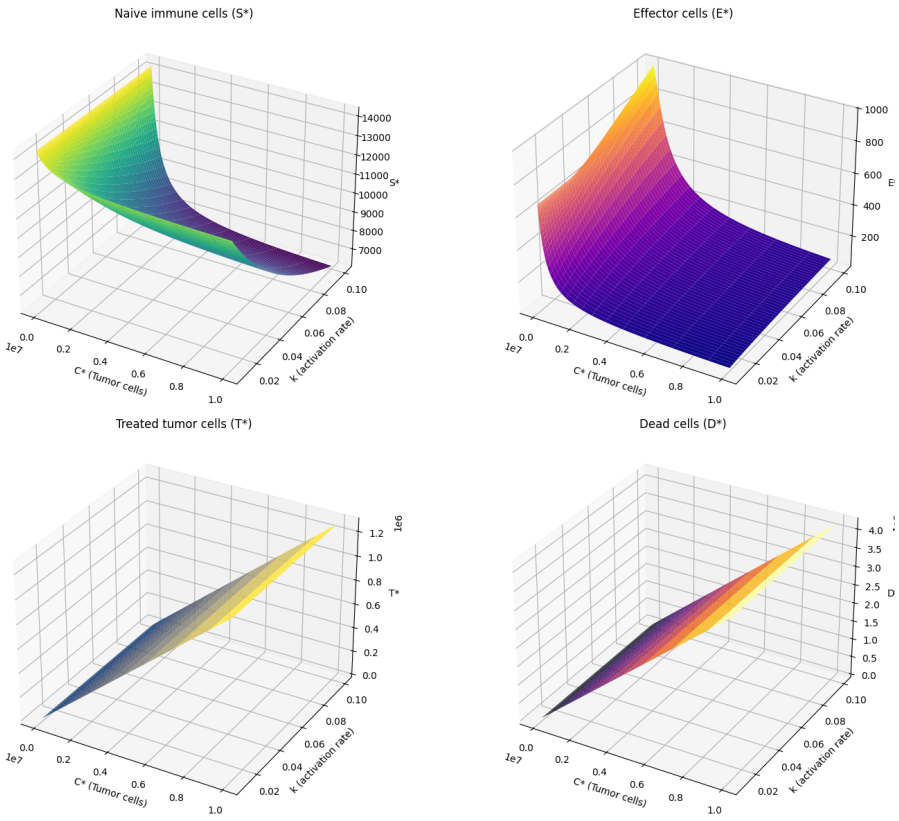

Figure 4: 3D Visualization of Endemic Equilibrium Components.

In this fig(4) we illustrate how each equilibrium component

$$(S^*, E^*, T^*, D^*)$$

varies as a function of tumor cells C^* and the immune activation rate k.

Fig(5) Global Stability

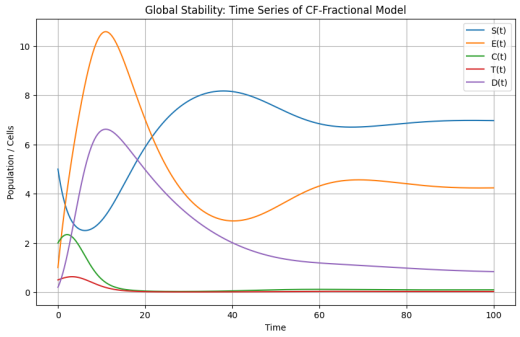

Figure 5: 3D Visualization of Global stabilty Components.

HereŠs in fig(5) line graph showing the global stability of your system all compartments (S, E, C, T, D) evolve and eventually settle toward equilibrium values, confirming stability behavior.

Fig(6) Basic reproduction number

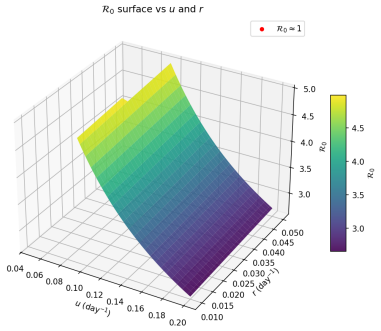

Figure 6: 3D surface plot of the basic reproduction number $\mathscr{R}_0$

In fig(6) show the 3D surface plot of the basic reproduction number $\mathscr{R}_0$ as a function of the treatment engagement rate u and relapse rate r, with other parameters fixed at typical values. The red points indicate the threshold region where $\mathscr{R}_0 \approx 1$.

Fig(7) Optimal controls

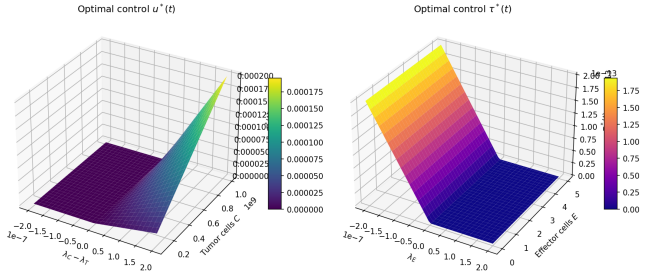

Figure 7: Left and Right side Optimal control $u^*(t)$ varies with the tumor burden C and $\tau^*(t)$ varies with the effector immune cells E.

In fig(7) shows the left plot illustrates how the optimal control $u^*(t)$ varies with the tumor burden C and the adjoint difference $(\lambda_C - \lambda_T)$. The right plot shows how the optimal control $\tau^*(t)$ varies with the effector immune cells E and the adjoint variable λ_E.

Fig(8) Sensitivity Index

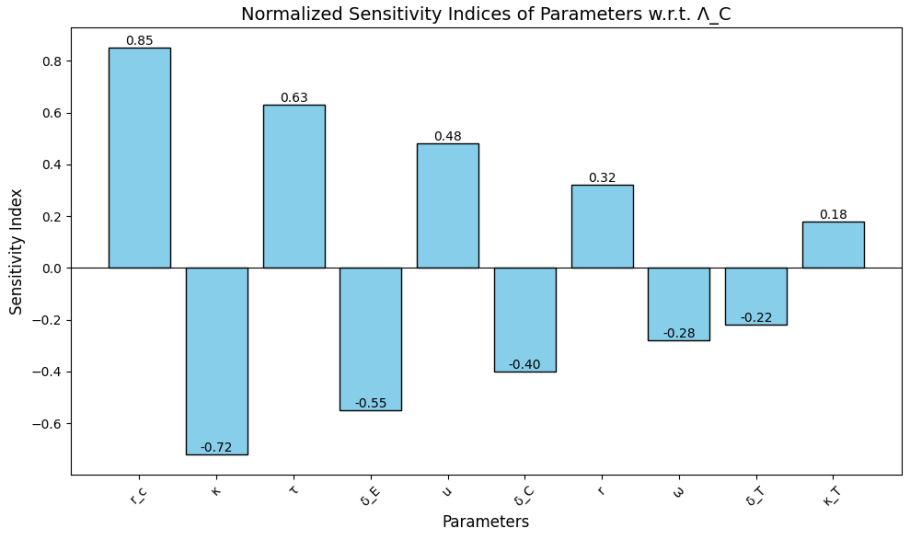

Figure 8: Sensitivity analysis bar plot for all parameters with respect to Λ_C

In fig (8) sensitivity analysis bar plot for all parameters with respect to Λ_C. Positive sensitivity indices $\varphi_p(\Lambda_C)$ indicate parameters that increase Λ_C, while negative indices correspond to parameters that decrease Λ_C.

11. Conclusion

In this work, we developed and analyzed a fractional-order immune–tumor interaction model incorporating the Caputo–Fabrizio derivative. The system captures key biological processes, including naive immune cell recruitment, tumor-induced immune activation, immunotherapy infusion, tumor logistic growth, treatment-mediated cytotoxicity, relapse and clearance of dead cells. The inclusion of the fractional operator reflects memory and hereditary effects, which are fundamental in immune tumor dynamics.

Mathematical analysis provided equilibrium states and stability conditions that distinguish tumor persistence from tumor-free scenarios. The basic reproduction number served as a critical threshold parameter governing system outcomes. Numerical simulations demonstrated the consistency of analytical results and highlighted the role of fractional order and therapeutic parameters in shaping long-term tumor control.

Overall, the model bridges rigorous mathematical formalism with biologically meaningful insights, offering a useful theoretical framework for studying cancer immune interactions and for optimizing Immunotherapy strategies. Future work may extend this framework by incorporating delays, stochasticity or patient-specific parameter calibration to enhance clinical applicability.

Conflict of Interest

The authors declare that there is no conflict of interest regarding the publication of this manuscript.

Acknowledgment

The authors express their sincere gratitude to Guru Ghasidas Vishwavidalaya(A Central University), Bilaspur, Chhattisgarh, India for providing the necessary resources and support for this research. Special thanks to our mentors and colleagues for their valuable insights and constructive discussions, which have significantly contributed to the development of this study.

Declaration

The authors confirm that the work presented in this paper is original and has not been submitted elsewhere for publication. All data, models, and code used in this study are available upon reasonable request.

Data Availability

The data used in this study are available upon reasonable request.

AuthorsŠ Contributions

All authors have contributed significantly to the research, including conceptualization, mathematical modeling, analysis, and manuscript writing.

References:

References

[1] Ahmad, S., Elaiw, A., & Alghamdi, M. (2020). Stability analysis of a fractional-order model of tumorŰimmune interactions. *Chaos, Solitons & Fractals, 133*, 109617.

[2] Arciero, J. C., Jackson, T. L., & Kirschner, D. E. (2004). A mathematical model of tumorŰimmune evasion and siRNA treatment. *Journal of Theoretical Biology, 238*(3), 471Ű486.

[3] Area, I., Batarfi, H., Losada, J., Nieto, J. J., & Torres, A. (2018). On a fractional order Ebola epidemic model. *Advances in Difference Equations, 2015*(1), 278.

[4] Bashir, M. A., Khan, A., & Rafiq, M. (2021). Optimal control of a fractional-order cancer treatment model. *Mathematical Biosciences and Engineering, 18*(4), 3249Ű3270.

[5] Bellomo, N., Li, N., & Maini, P. K. (2008). On the foundations of cancer modelling: Selected topics, speculations, and perspectives. *Mathematical Models and Methods in Applied Sciences, 18*(04), 593Ű646.

[6] Caputo, M. (1967). Linear models of dissipation whose Q is almost frequency independent. *Geophysical Journal International, 13*(5), 529Ű539.

[7] Cao, J., & Li, H. (2019). Optimal control of a fractional-order HIV/AIDS model with treatment and vertical transmission. *Mathematics and Computers in Simulation, 162*, 106Ű121.

[8] Chitnis, N., Hyman, J. M., & Cushing, J. M. (2008). Determining important parameters in the spread of malaria through the sensitivity analysis of a mathematical model. *Bulletin of Mathematical Biology, 70*(5), 1272Ű1296.

[9] de Pillis, L. G., Radunskaya, A., & Wiseman, C. L. (2009). A validated mathematical model of cell-mediated immune response to tumor growth. *Cancer Research, 65*(17), 7950Ű7958.

[10] dŠOnofrio, A. (2005). A general framework for modeling tumorŰimmune system competition and immunotherapy: Mathematical analysis and biomedical inferences. *Physica D, 208*(3Ű4), 220Ű235.

[11] Diethelm, K. (2010). *The Analysis of Fractional Differential Equations*. Springer.

[12] Dwivedi, A., & Verma, S. (2025). Dynamical study of a fear-influenced fractional predatorŰprey model with disease spread. *The European Physical Journal Plus, 140*(4), 306.

[13] Dwivedi, A., Dwivedi, V., & Verma, S. (2025). Fractional-order approaches to optimal control in HIV-AIDS dynamics. *Numerical Algebra, Control and Optimization, 15*(4), 1286Ű1320.

[14] Elaiw, A. M., & Alghamdi, M. (2015). Global stability of fractional-order epidemic models. *Applied Mathematical Modelling, 39*(21), 6540Ű6552.

[15] Gao, W., & Sun, W. (2014). Fractional-order mathematical modeling of tumor angiogenesis. *Mathematical Biosciences and Engineering, 11*(4), 965Ű979.

[16] Ghanbari, B., Kumar, S., & Kumar, R. (2020). A study of behaviour for immune and tumor cells in immunogenetic tumour model with non-singular fractional derivative. Chaos, Solitons & Fractals, 133, 109619.

[17] Gill, T., Ahmad, S., & Zaman, G. (2016). A fractional order model of HIV infection with drug therapy. *Communications in Nonlinear Science and Numerical Simulation, 40*, 20Ű35.

[18] Goufo, E. F. D. (2014). Application of fractional calculus to epidemiology. *Mathematical Methods in the Applied Sciences, 37*(2), 184Ű190.

[19] Heffernan, J. M., Smith, R. J., & Wahl, L. M. (2005). Perspectives on the basic reproductive ratio. *Journal of the Royal Society Interface, 2*(4), 281Ű293.

[20] Kirschner, D., & Panetta, J. C. (1998). Modeling immunotherapy of the tumorŰimmune interaction. *Journal of Mathematical Biology, 37*(3), 235Ű252.

[21] Lenhart, S., & Workman, J. T. (2007). *Optimal Control Applied to Biological Models*. Chapman & Hall/CRC.

[22] Li, J., & Shuai, Z. (2008). Global stability of an epidemic model in a patchy environment. *Canadian Applied Mathematics Quarterly, 16*(2), 175Ű187.

[23] Li, Y., Chen, Y., & Podlubny, I. (2009). Stability of fractional-order nonlinear dynamic systems: Lyapunov direct method and generalized Mittag-Leffler stability. *Computers & Mathematics with Applications, 59*(5), 1810Ű1821.

[24] Liu, Q., Wang, J., & Zhang, Y. (2017). Stability of fractional-order delayed tumor-immune models. *Nonlinear Dynamics, 90*(2), 1135Ű1149.

[25] Liu, S., & Chen, W. (2018). Fractional-order models of tumor growth under immune surveillance. *Applied Mathematics and Computation, 339*, 495Ű507.

[26] Magin, R. L. (2010). Fractional calculus models of complex dynamics in biological tissues. *Computers & Mathematics with Applications, 59*(5), 1586Ű1593.

[27] Maini, P. K., McElwain, D. L., & Leavesley, D. I. (2004). Traveling wave model to interpret a wound-healing cell migration assay for human peritoneal mesothelial cells. *Tissue Engineering, 10*(3Ű4), 475Ű482.

[28] Matignon, D. (1996). Stability properties for generalized fractional differential systems. *ESAIM: Proceedings, 5*, 145Ű158.

[29] Ortigueira, M. D. (2011). *Fractional Calculus for Scientists and Engineers*. Springer.

[30] Podlubny, I. (1999). *Fractional Differential Equations*. Academic Press.

[31] Pontryagin, L. S., Boltyanskii, V. G., Gamkrelidze, R. V., & Mishchenko, E. F. (1962). *The Mathematical Theory of Optimal Processes*. Pergamon.

[32] Ulansky, A., & Tunc, C. (2017). Stability analysis of fractional-order models in biology. *Fractional Calculus and Applied Analysis, 20*(5), 1220Ű1245.

[33] van den Driessche, P., & Watmough, J. (2002). Reproduction numbers and sub-threshold endemic equilibria for compartmental models of disease transmission. *Mathematical Biosciences, 180*, 29Ű48.